ACS APPLIED NANO MATERIALS

www.acsanm.org Article

Rapid, General-Purpose Patterning of Silicon Nitride Thin Films Under Ambient Conditions for Applications Including Fluid Channel and SERS Substrate Formation

Brian S. Sheetz, Y.M. Nuwan D.Y. Bandara, Benjamin Rickson, Michael Auten, and Jason R. Dwyer*

Cite This: *ACS Appl. Nano Mater.* 2020, 3, 2969–2977 Read Online

ACCESS | Metrics & More | Article Recommendations | Supporting Information

ABSTRACT: Silicon nitride thin films are useful as etch-stop masks in micro- and nanofabrication. As structural elements, they are prevalent in applications as diverse as single-molecule sensing, transmission electron microscopy, ultrafast spectroscopy, superfluidity studies, and high flux liquid filtering. A hand-held "flameless" Tesla-coil lighter was used to create vias through 200 nm silicon nitride (SiN_x) films coating silicon wafers. The processing allowed spatially directed KOH etching of the underlying Si. Patterning could be achieved with a hard mask or rastering of the spatially confined discharge, offering—with low barriers to rapid use—particular capabilities that might otherwise be out of reach to researchers without access to conventional, instrumentation-intensive micro- and nanofabrication workflows. General patterning capabilities were demonstrated, followed by the formation of a trench suitable for microfluidic applications. Finally, a discharge-treated thin film surface was sputter coated with gold to create a surface enhanced Raman spectroscopy (SERS) substrate that was then used to detect a test analyte at ppm concentration.

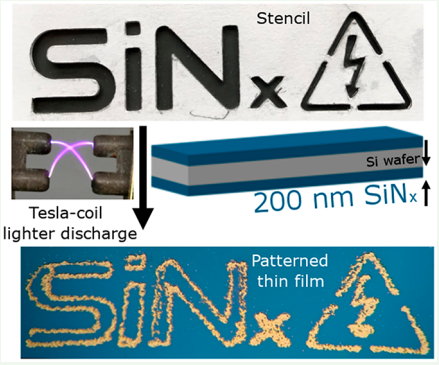

KEYWORDS: *silicon nitride, thin film, Tesla-coil, patterning, microfabrication, nanofabrication, vias, surface enhanced Raman scattering (SERS)*

INTRODUCTION

Thin-film silicon-rich silicon nitride films (SiN_x) have become ubiquitous in consumer electronics and in platforms across the sciences and engineering. These thin films serve a wide range of functions in micro- and nanofabricated processes and products, and in their applications, including as simple structural building blocks; as barriers serving as electrical insulation, sample supports and sample chamber windows, diffusion barriers, chemical etch stops, and surface passivation layers; and as the foundation for more sophisticated (nano)-structures.[1−11] SiN_x-coated Si wafers can be purchased commercially so end users therefore need neither access to the specialized infrastructure of nanofabrication nor operational expertise. Only slightly more complicated nanofabricated structures—free-standing ∼100 nm-thick SiN_x "windows" on Si frames—are available commercially after a tightly controlled series of photolithographic, reactive ion etching (RIE), and wet chemical etching steps in clean rooms with suitable equipment.[1,2,5,6] Such windows have a host of applications including as sample supports that provide effective transparency to charged particles and photons across a range of energies; as windows to interface instrumentation operating in vacuum to samples in ambient or liquid environments; supporting nanopore single-molecule sensors for genomics, proteomics, and glycomics; and housings for nanoapertures for filtration and controlled sample introduction and formation.[1,6,12−20]

Without access to a vendor or to suitable nanofabrication facilities and equipment, even such a simple, yet powerful, structural modification of a SiN_x-coated Si wafer would be essentially out of reach. The very benefits of SiN_x thin films for such applications listed above—their mechanical, electrical, and chemical robustness—can prove quite burdensome when modifying their structure.

The use of a lithographically- and RIE-patterned SiN_x thin film as a hard mask for subsequent processing, as in the fabrication of the free-standing windows described above, is an important approach in Si micro- and nanofabrication more generally. In this embodiment, a SiN_x thin film is deposited onto each side of the Si wafer: one of the films is sacrificed to be patterned as a hard mask to spatially control a wet etching process, and the other film is protected so that it remains intact across the opening created by removal of Si. A conventional fabrication flow, carried out in a clean-room housing the necessary instrumentation, involves (1) spin-coating a thin film

Received: January 28, 2020
Accepted: March 4, 2020
Published: March 4, 2020

https://dx.doi.org/10.1021/acsanm.0c00248
ACS Appl. Nano Mater. 2020, 3, 2969–2977

Scheme 1. Implementations to Selectively Damage SiN_x-Coated Si Wafers with a Tesla-Coil Lighter Discharge, Including Patterning for Subsequent Wet Etching[a]

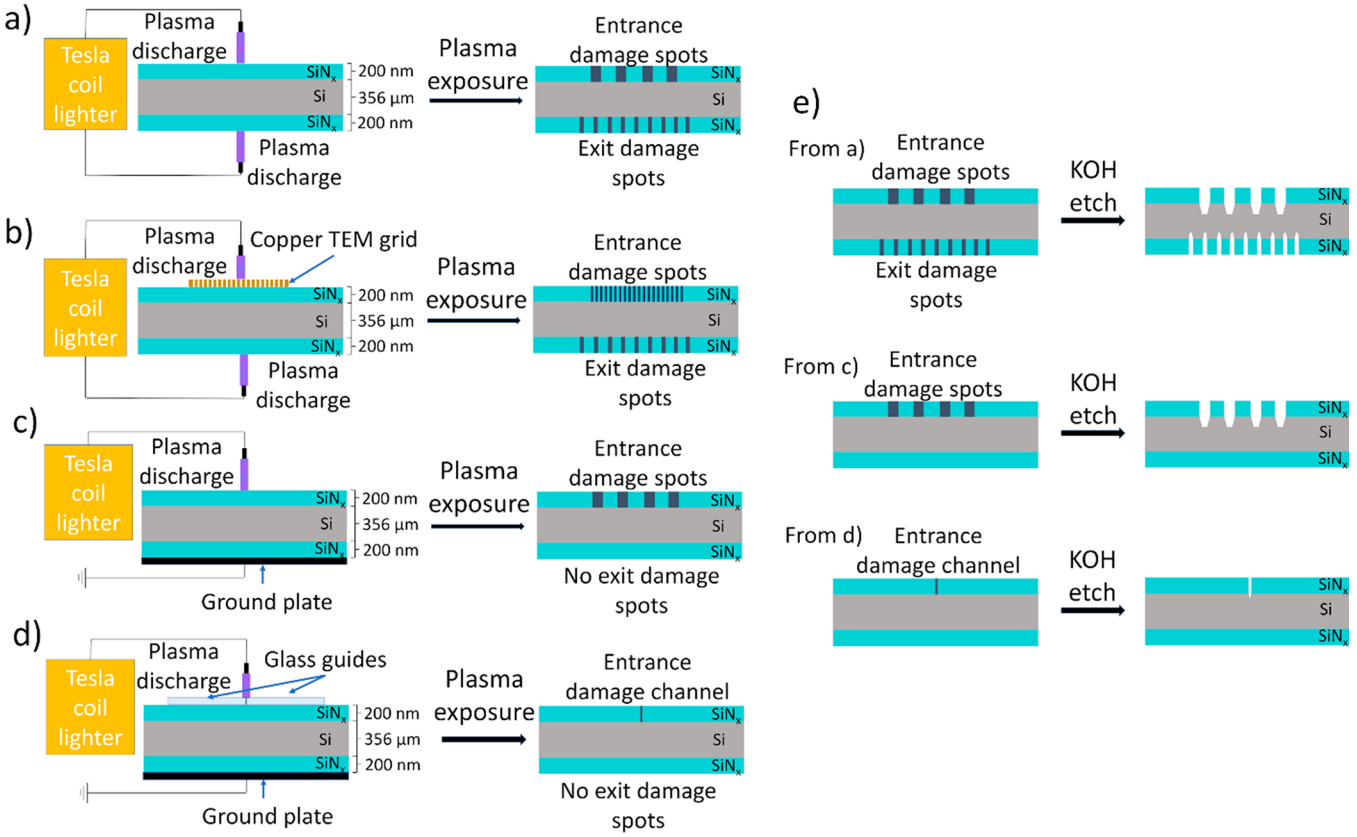

[a](a) Direct, unmodified wafer exposure; (b) Patterned exposure through a copper grid mask; (c) Direct exposure with a grounded bottom plate; (d) Channel formation between glass slide masks; and (e) Wet KOH etch outcomes after specified Tesla-coil exposures. Thicknesses of SiN_x films and Si wafers are not drawn to scale.

of (polymer) photoresist onto both SiN_x films; (2) photo-irradiating one photoresist layer through a mask to transfer the mask pattern to that photoresist layer; (3) selectively dissolving away the parts of the photoresist that had been exposed to light (or those that had been shielded from light exposure by the mask); (4) transferring the piece to a vacuum chamber where reactive gases then etch away (by RIE) the now-exposed areas of SiN_x, (5) leaving the protective photoresist layer intact and the still fully photoresist-coated SiN_x layer untouched; (6) removing the remaining photoresist layers; and (7) finally subjecting the Si exposed through openings in the now-patterned SiN_x layer to whatever material processing steps were the end goal of this work flow, etching by immersion in a hot KOH bath for the formation of free-standing SiN_x windows. In this example, one SiN_x film coating the wafer is sacrificed to use as a mask, and the other is left intact to serve as the window over a micrometer to millimeter-length scale opening. Importantly, all of this intensive materials processing does not necessarily yield a single nanoscale feature: it simply relies on the existing nanoscale thickness of the SiN_x film. In other words, all of the nanoscale fabrication was done only during the SiN_x thin film deposition stage. Given the complexity, duration, and equipment necessary to arrive at even this single desired processing step (spatially localized KOH etching), we were interested in developing a new method to permit structural modification of as-supplied SiN_x thin films quickly and without the need for specialized facilities.

Such a capability would allow the patterning of SiN_x thin films as a stand-alone goal, as well as the patterning of SiN_x thin films to serve as masks for further processing of an underlying substrate. Mechanical options, such as use of a diamond scribe, could work for supported films, but we sought a noncontact route to allow for modification of free-standing SiN_x films. An alternative to mechanical damage by scribing might also allow for more flexible patterning using masks. Wet chemical etching of SiN_x can be done on the benchtop using hydrofluoric acid and, less commonly, using hot phosphoric acid (both approaches require specialized labware for safety),[5,21] but would require an initial photolithography step for spatial control over material removal, and may still be compromised by the inability to anisotropically etch the amorphous SiN_x. Given the demonstrated ability of a hand-held Tesla-coil (flameless) lighter to form nanofluidic conductors in free-standing SiN_x immersed in deionized, ultrapure water by dielectric breakdown-initiated material removal,[13,22] we hypothesized that the same device could provide the means to directly pattern, on a larger-scale, thin films of SiN_x, without need for additional processing or hardware, and without physical contact of the tool to the piece. We, moreover, hypothesized that the approach could offer the additional benefit of replacing, with a single operation, steps (1)−(6) of the example SiN_x microfabrication process outlined above. Scheme 1 outlines the proposed processing steps. Dielectric breakdown, charging, thermal effects, and electron-beam-

https://dx.doi.org/10.1021/acsanm.0c00248
ACS Appl. Nano Mater. 2020, 3, 2969−2977

driven surface chemistry in air may all play a role in any observed material processing.[13,22,23] Given that the preexisting ~100 nm thickness of the SiN_x films would be the "nano" element of this fabrication challenge, we were unconcerned that the ~100 μm diameter of the Tesla-coil lighter beam was not expected to offer high lateral resolution. The proposed Tesla-coil lighter-based method is thus akin to the earlier example of photolithography, RIE, and wet chemical etching used to produce a free-standing SiN_x window: neither produces new nanoscale features, but rather both rely on thin-film deposition to create structures with the desired nanoscale dimensions.

Beyond exploring the capacity of the Tesla coil lighter method to perform thin film patterning, we targeted two applications. The first was the use of Tesla-coil-patterned SiN_x as a hard mask to create a microfluidic channel in the underlying silicon wafer by wet chemical etching. The second was to use Tesla-coil-modified thin film substrates as a foundation for the fabrication of a substrate for surface-enhanced Raman spectroscopy (SERS). There is precedent for the use of SiN_x-coated wafers as a base layer for SERS substrates created by straightforward, low-barrier electroless plating,[24] but the use of the Tesla coil has the potential to introduce a patterned enhancement without the need for preliminary patterned monolayer formation.[25] Raman enhancement is provided by substrates that are structured on the nanoscale and considerable effort has been devoted to optimizing both the fabrication and sensing performance of SERS substrates. Top-down nanofabrication steps can yield exquisitely structured substrates, but rely on intensive and expensive fabrication steps.[26−32] We chose to use commercially available Silmeco SERS substrates as a benchmark to test the performance of our simple approach. These substrates consist of metallized high aspect ratio silicon nanopillars—with tunable dimensions, for example, <100 nm in diameter and ~1 μm long—that can tilt together during solvent evaporation to form (self-assembled) SERS hot spots.[30,33] These nanopillars are produced by maskless RIE followed by a variety of preparation and deposition steps.

EXPERIMENTAL SECTION

Silicon nitride-coated wafers were purchased from Rogue Valley Microdevices, Inc. (Medford, OR), and consisted of 200 nm-thick, low-stress (<250 MPa Tensile; silicon-rich), LPCVD SiN_x films deposited on double-polished, 356 ± 25 μm-thick, 3" diameter, <100> polished, P/Boron-doped (1−20 Ω·cm resistivity) silicon wafers. Flameless Tesla-coil lighters were purchased from Tesla Coil Lighters: single arc (ASIN: B016P8A1K4/UPC: 849344046936/model H&PC-64671) and dual arc (ASIN: B01A02F714/UPC: 849344050544/Item model number: H&PC-65026). A custom jig was 3D printed to accurately and reproducibly position the wafer relative to the lighter terminals. TEM grids (G50-Cu, G200-Cu, G400-Cu) were purchased from Electron Microscopy Sciences (Hatfield, PA 19440). Semiconductor grade potassium hydroxide (99.99% trace metals basis, product no. 306568), anhydrous acetonitrile (99.8%, product no. 271004), and 4-nitrothiophenol (technical grade, 80%, N27209; abbreviated NBT) were purchased from Sigma-Aldrich (now Millipore Sigma, St. Louis, MO). Raman spectra were acquired with a Snowy Range Instruments, Sierra 2.0 spectrometer operating at 785 nm and 100 mW, with its orbital raster scanning mode disabled. Benchmark SER spectra were recorded using a gold SERS substrate from Silmeco ApS (Copenhagen, Denmark). SERS substrates were soaked in 1.6 ppm solutions of 4-nitrothiophenol in acetonitrile for 5 min before being removed and air-dried after wicking excess liquid away with a Kimwipe. Electron micrographs were recorded using a Zeiss SIGMA VP field emission-scanning electron microscope (FE-SEM) and gold coatings were deposited for 20 s using a Cressington 108 Auto gold sputter coating system operated at 30 mA currents during deposition.

Insertion of the double-sided SiN_x-coated Si chips between the terminals of the Tesla coil lighter (Scheme 1a) did not prevent transmission of the discharge-path "flame", and resulted in visible discoloration of the chips spatially localized to where the "flame" passed, as shown in Figure 1. Two different damage patterns could be

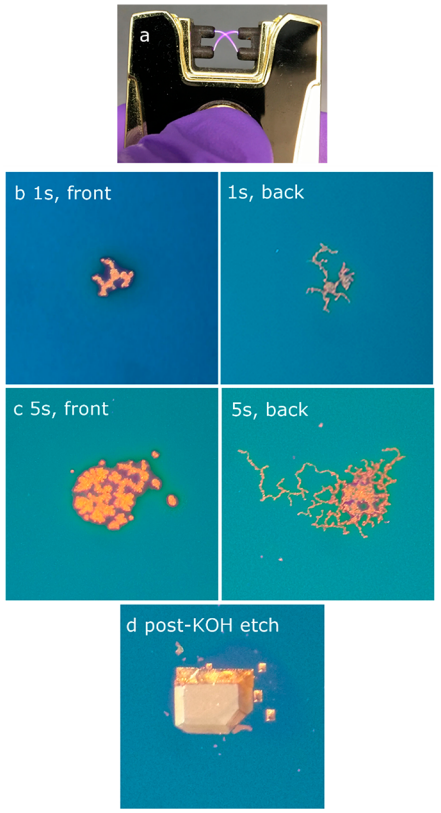

Figure 1. a) A four-electrode Tesla-coil lighter, with dual discharges. Damage spots resulting from (b) 1 s and (c) 5 s exposures to the Tesla-coil, with frames sized to 15 mm × 15 mm. The images in the left and right columns are taken from opposite sides of the SiN_x double-coated chip. Image (d) shows the result of 30 min of KOH etching of the front damage spot in (c).

identified, consistently depending on whether the lighter discharge was incident upon the SiN_x through air (entrance face; fairly well-defined spots), or through the Si wafer (exit face; more dispersed, thread-like damage tracks). The character of the two types of spots could be readily understood in a mean-free-path framework. While the incident discharge always appeared spatially confined as a filament, some instability in the discharge path could be detected by eye. This "wandering" made the degree of localization of the damage dose-dependent, with longer exposure times allowing a greater degree of infilling of the still localized damage spot. Supporting Information (SI) Figure S1 shows electron micrographs of two entrance face damage spots that show that the damage depth increased with exposure time, and on a micrometer length scale exceeding the thickness of the thin SiN_x film. The Tesla-coil discharge produced a highly textured (pebbled), ostensibly porous, layer that had a clear lower boundary with an appreciable extent of the underlying silicon wafer that showed no microscopic evidence of material damage. SI Figures S2 and S3 illustrate that the damage spots at short exposure times were formed from isolated damage tracks traversing regions of intact SiN_x film. The lower degree of damage spot infilling and greater lateral extent of travel of the damage tracks with greater distance from

https://dx.doi.org/10.1021/acsanm.0c00248
ACS Appl. Nano Mater. 2020, 3, 2969−2977

electrode to film at this short exposure time was consistent with projection of the angular fluctuations onto the film surface. Beam path fluctuations would thus complicate—by separation-dependent projection of angular deviations and consequent dwell time/unit area fluctuations, for example—any effort to study the effect of distance between electrode and thin film, so we do not systematically explore the parameter here. The degree of homogeneity of the damage spots was increased with longer (10 and 30 s) exposure times, as shown in SI Figure S3. SI Figure S3 also reveals that the SiN_x thin film inside the damage spots was intact outside of the damage tracks. Cross-sectional imaging revealed that the damage tracks penetrated on the micrometer length scale into the underlying silicon of the wafer, forming divots, with no visible evidence of intact SiN_x film remaining. Elemental analysis revealed that the Tesla-coil-induced damage is not merely physical, but is accompanied by chemical changes, as well. EDX analysis of damage spots in SI Figures S4 and S5 showed compositional changes at the damage spot relative to intact SiN_x film. A decrease in nitrogen content was accompanied by an increase in oxygen content. The spatial distribution of this chemical change overlapped with the visible extent of the damage spot, with the underlying undamaged region comprised of chemically unmodified silicon. Damage tracks formed by the Tesla-coil lighter were thus demarcated by pitting of the Si wafer, formation of a convoluted overlayer, and local chemical changes.

Our motivation was not simply that we could spatially damage the SiN_x using a Tesla-coil lighter, though, but that (1) the damaged spot could be trivially processed to provide access to the material underlying the damage; and (2) the ostensibly undamaged regions of the SiN_x thin film could be used to protect the underlying material in those regions. In essence, that the SiN_x film exposed to the lighter could serve as a hard mask for patterning the wet-etching of the underlying Si wafer (Scheme 1e). Well-established within the canon of micro- and nanofabrication techniques, an intact SiN_x film serves as a KOH etch stop and should protect the underlying Si from etching (except at unprotected edges).[1,5,6] We were able to KOH etch even the shortest duration damage spots that we tested. Figure 1 shows the formation of a KOH etch pit where the Tesla-coil (5 s exposure) had visibly discolored the SiN_x film. The etch pit profile is consistent with anisotropic KOH etching of the underlying crystalline Si (here, 30 min in an ~8.9 M KOH solution at ~80 °C). The etch pit formed where the initial Tesla-coil damage spot had been evident, with no additional processing carried out, and the etching process "filled-in" the fine structure present in the damage spots, possibly due to KOH etching of less evidently damaged areas of the SiN_x between the damage tracks, or merging of adjacent etch pits, or both. Regardless of mechanism, the combination of Tesla-coil-exposure and KOH etching produced an etch pit at a specific location and with spatially limited margins. Thus, while the discharge path fluctuated, unexposed regions of the thin film were unharmed and patterning of the SiN_x film could be used to (1) pattern a 200 nm thin-film structure and (2) govern patterning of the underlying structure: the method thus offers demonstrable capabilities as a rapid, low-barrier alternative to lithography, demonstrated on a thin film material often chosen for its resistance to removal.

Following the demonstration that the Tesla coil lighter could induce damage to the SiN_x thin film that was compatible with subsequent processing and structuring of the underlying substrate, we wanted to explore to what extent we could pattern the damage to the film. We attempted two different routes to patterning: (1) patterning through a physical mask (Scheme 1b), and (2) contactless patterning by translating the lighter through defined paths. In the first case, we placed flexible copper grids used as sample supports for transmission electron microscopy (TEM), shiny-side down against the chips, albeit without guarantee of uniform grid contact to the film across the grid diameter or lateral immobility. The two-terminal Tesla-coil lighter was used here to offer a single discharge path, and the images in Figure 2 were taken from the entrance film side, the side proximal to the terminal that would produce well-defined spots in the absence of a mask (see Figure 1). Exposure times did not exceed ~30 s, and the Tesla-coil was manually passed over the entire grid area, with

Figure 2. In the left column, the illumination was configured to image all surface features. In the right column, the optical axis of the camera was orthogonal to the surface and illumination was direct so that only scattered light would be imaged. Scale bars are 0.5 mm. From top to bottom, the SiN_x chips were masked with a 400, 200, and 50 mesh copper TEM grid (Scheme 1b).

fluctuations in the discharge path itself providing additional spatial sampling across the grid. Complete and uniform coverage is not expected given this crude approach to spatial sampling. The copper mask offers two properties to an electric-discharge-based patterning method: density, and conductivity. The conductive mask is on top of an insulating thin film with the discharge able to transmit through the entire wafer and also able to damage the thin film with increasing exposure time (Figure 1). Thus while the copper grid is electrically floating at the beginning of the exposure, the electrical potential on the grid is likely variable in complex ways during the course of the exposure. In SI Figure S6, we show photographs of two grids before and after use as masks: there is evident discoloration, suggesting damage, to the copper masks by the Tesla-coil discharge. With high-field electric discharges, the role of microscopic asperities may further complicate transient electric field distributions and allow for localized discharges accompanied by microscopic losses of grid material. The images shown in Figure 2 are the best results from a number of repeated trials, and while the implementation requires optimization, we emphasize two points. First, the physical masking was able to control the Tesla-coil patterning. Second, the variation in damage pattern with mesh size—50 mesh (420 μm hole, 80 μm bar), 200 mesh (90 μm hole, 35 μm bar), and 400 mesh (37 μm hole, 25 μm bar)—offered an interesting trend. The 50 mesh, with large open area,

https://dx.doi.org/10.1021/acsanm.0c00248
ACS Appl. Nano Mater. 2020, 3, 2969−2977

showed that the damage was localized to the grid bars, principally underneath the bars but also extending outward from them. In the 200 mesh patterning the damage underneath the bars was limited in extent compared to the damage in the open areas. Nevertheless the central portion of the thin film underneath each grid opening was largely undamaged in this mesh size, suggesting that the damage was originating not by direct bombardment of the Tesla-coil discharge, but from discharge from the grid. In the 400 mesh patterning, the damage spots appeared to be infilled underneath the openings in the grid, but largely absent underneath the wires. Thus, patterning of the damage spots using this mask is complicated by its conductivity, and likely by edge and proximity effects, but transfer of grid features is nevertheless feasible. We did not explore the limit on achievable lateral feature size but possible beam-induced damage to masks with small bars, especially, and crosstalk between closely spaced bars will likely be important, and limiting, considerations. The focus of the fabrication effort, however, was to augment, by even microscale patterning, the nanoscale vertical feature size given by the 200 nm film thickness. While the implementation requires optimization, most likely in ensuring uniform contact of the grid to the SiN_x thin film and preventing lateral displacement during patterning, this proof-of-principle demonstration of the use of a physical mask for pattern transfer was clearly promising.

Our more significant interest than using a hard mask for patterning the SiN_x was exploring whether the spatially confined discharge of the Tesla-coil lighter could be used for patterning by rastering. The compact, hand-held Tesla-coil lighter allows for freeform patterning, but we wanted to produce patterns without using a mask and that would be smaller than could readily be produced by hand, and so we used a pantograph to reduce the pattern scale 4-fold. We attached one end of the pantograph to the Tesla-coil lighter and the other end to a stylus confined within a paper cut-out stencil. The Tesla coil terminals were placed on either side of the wafer section without making contact (as in Scheme 1a), and the stylus tip was in contact only with the stencil. The stylus was used to trace the stencil pattern, and the pantograph caused the Tesla-coil lighter to replicate this motion, although with purposefully 4-fold reduced travel. The use of a stencil allowed for us to explore rastering-based patterning that would not be limited by the practitioner's manual dexterity, and that would allow for repeated coverage of the same area to be patterned. There was an additional benefit of the use of the pantograph to reduce the pattern size, and that is that the slower speed of travel of the lighter compared to the tracing stylus was expected to aid in creating contiguous damage tracks. Figure 3 shows an image of the stencil; the stylus diameter allowed for the pattern on the SiN_x to be traced as an outline, as shown in the three photographs below the stencil. The damage line across the middle of the traced "S" at the 11 o'clock position resulted from displacement of the stylus away from the edge of the stencil and shows the possibility of patterned film modification also by infilling. The KOH etching (Scheme 1e) was carried out for 10 min, and slightly broadened the spatial extent of the visible damage, improving the contiguousness of the structural modification of the film (Figure 3).

In Figure 1 we demonstrated a difference in the damage spot quality between the entrance and exit faces of the wafer section. On the entrance side the spots were better defined, and on the exit side the spot integrity was diminished. The same general behavior was observed in the patterning experiments. It was difficult to discern exit-face patterning when using the copper grid masks, owing to the small feature size of the masks, the rudimentary implementation, and the inherent differences in entrance and exit face damage spot quality and extent. For the raster-based, mask-free patterning, the exit face pattern quality was also distinct from the entrance face quality, but with the overall pattern remaining clear. Figure 4 illustrates that the exit face damage marks had two prominent zones: a sharply defined set of damage marks surrounded by a more diffuse halo. The asymmetric patterning quality between entrance and exit faces is a concern only in those special applications where both films must be patterned. SiN_x thin films are conventionally deposited in one fabrication step onto both sides of a wafer even when only one side will be used as a patterned mask (as in the SiN_x window formation example enumerated above) or structural element. Thus, the ability here to robustly pattern only the entrance thin film is not inherently a

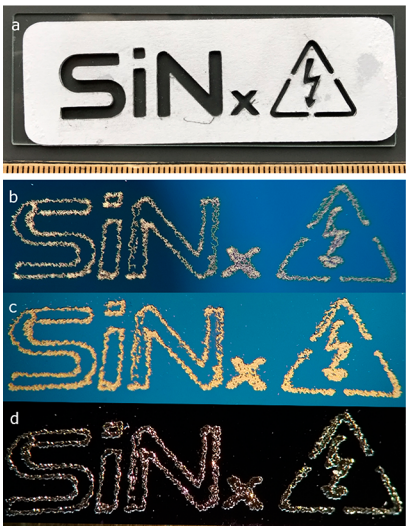

Figure 3. (a) A cut-out paper stencil (1 mm ruler markers) was traced using a pantograph to provide ~4× reduction in scale to the corresponding pattern induced on SiN_x-coated wafers using a Tesla-coil lighter. The chip with (b) as-generated damage spots was (c) etched in KOH for 10 min, with image illumination in (c) and (d) corresponding to the left and right columns of Figure 2.

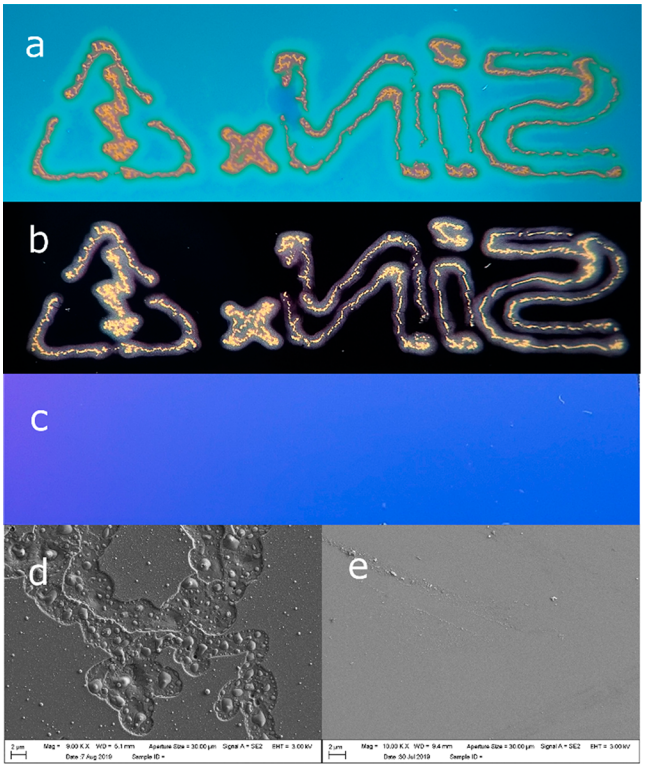

Figure 4. Exit-side patterning of SiN_x under (a,b) the two image lighting conditions of Figure 2. A central prominent set of damage marks is surrounded by a diffuse halo. In (c), a grounding plate was placed against the exit side of the wafer being patterned, eliminating all visible indications of exit damage. The electron micrograph in (d) shows exit face damage marks generated without a grounding plate (as in Scheme 1a), and (e) shows the exit face in the presence of the grounding plate (as in Scheme 1c).

https://dx.doi.org/10.1021/acsanm.0c00248
ACS Appl. Nano Mater. 2020, 3, 2969−2977

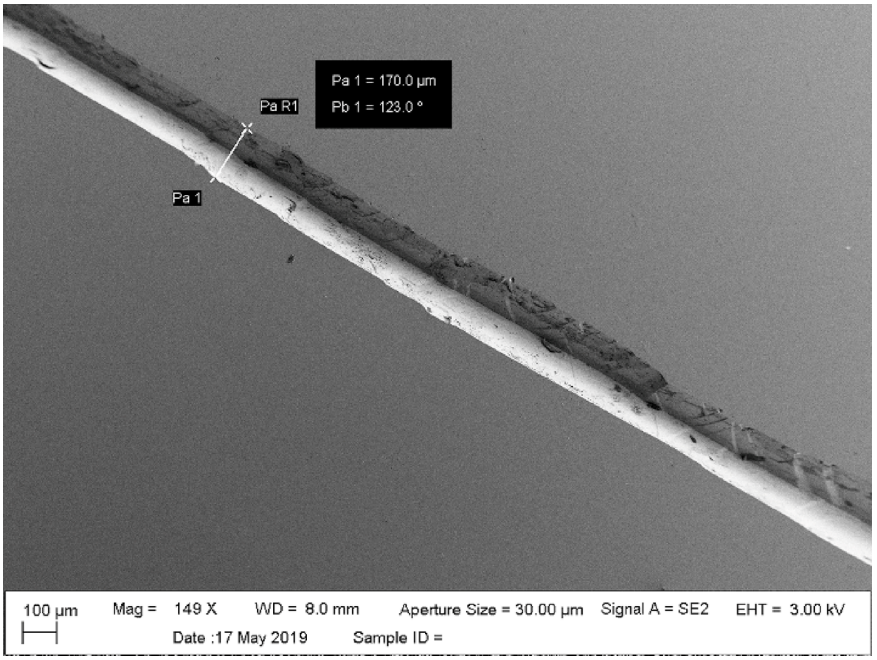

Figure 5. SEM images of a wet-etched (30 min in 8.9 M KOH at 80 °C) microchannel patterned by Tesla-coil discharge through the gap between two abutted glass slides.

limitation. We show two applications, below, where any damage to the exit film is irrelevant to the function arising from the entrance film patterning. Nevertheless, we also show in Figure 4c that it is possible to prevent visible damage to the exit side film by placing a grounded plate against it, here a microscope slide wrapped in aluminum foil connected by wire to an electrical outlet ground (Scheme 1c). In this case, damage was observed on the entrance face of the wafer of interest, but not on the exit face. Figure 4d and e show electron micrographs that illustrate the ability of the grounding plate to suppress the formation of even microscopic damage marks on the SiN_x film of the exit side. While the entrance face could be etched with KOH, there was no etching visible on the exit face, thus further indicating an absence of damage to the exit face SiN_x thin film.

Extension of the patterning shown in Figure 3 can be used to form functional elements such as fluid channels in the silicon wafer. Here, we implemented this by taping two clean glass microscope slides with their longer edges flush with each other, thereby providing a very thin guide channel. The wafer was placed onto the grounded backing plate as in the setup to Scheme 1d (and Figure 4c) and the free electrode was passed back and forth along the guide channel while discharging, at a manual scan rate of ∼1 cm/s. The damaged substrate was then placed into an 8.9 M KOH etch bath at 80 °C for 30 min (Scheme 1e) to produce the fluid channel shown in Figure 5. The walls of the channel are angled, meeting at an apex at the bottom, consistent with anisotropic KOH etching of the <100> polished Si wafer. The SEM image is thus slightly angled relative to the viewer. EDX analyses in SI Figure S7 are consistent with formation of the fluid channel in a region free of SiN_x thin film. The best control over the channel quality was achieved when the glass guide slides were making good contact with the substrate. The channel dimensions were 170 μm across and 160 μm deep, with the depth set by the etching duration. There was no need to take precautions to protect the exit face SiN_x film from being damaged because the desired feature never reached that side of the wafer.

Electron micrographs of the entrance surface post-Tesla-coil treatment in Figure 6 revealed dramatic surface roughening and the formation of features from pores to grains, with grain size distribution across a range of length scales. The Tesla coil treatment thus could produce entrance surface patterning on two broad length scale classes: on the dimension of the discharge and how far it was translated, and the microscopic length scales seen in Figure 6. In terms of applications, planar, polished SiN_x thin films have previously been used to support nanostructured gold films that provide the necessary enhancement for SERS.[24] The highly structured damaged surface in Figure 6 provides features (1) on length scales that could be leveraged for providing enhancement for SERS and (2) with high local surface area that can be beneficial for SERS. We sputter-coated the processed substrates with gold, where the resulting essentially featureless gold films allow any enhancement to be dominated by the underlying morphology of the damage spot. Indeed, control studies confirmed the expected results that the SERS signal was generated only by the combination of damage and gold coating, not either in isolation. In extension of this, the Tesla-coil could be used to create SERS-active regions of the substrate surrounded by undamaged regions without enhancement, as tested by direct SERS measurement. This spatially patterned enhancement was achieved by a uniform gold deposition step, subject to line-of-sight effects, of a thin gold layer across the entire surface where the only patterning was provided by the Tesla-coil damage. The patterned response was straightforward to achieve by Tesla-coil treatment of the SiN_x-coated chips, as opposed to the greater procedural complexity required to achieve spatially localized enhancement by a method such as patterned electroless deposition.[24,25] The ease of SERS substrate fabrication by Tesla-coil was even more marked compared to the fabrication of the highly refined, nanopillar-array-decorated, commercially available Silmeco SERS substrate. Using the same 1.6 ppm solution of our NBT test solution, we were able to record SER spectra of comparable quality from the commercial and extemporaneous substrates. Aside from the ability to so easily control the optical performance of the substrate, there may be more general uses of the fabrication paradigm of patterning a base layer followed by a spatially uniform deposition step.

■ CONCLUSIONS

We have demonstrated that a hand-held "flameless" Tesla-coil lighter produces spatially localized damage of thin (200 nm) SiN_x films on a Si wafer, that this damage spot provides wet chemical access to the underlying Si that allows further material processing, and that the remainder of the SiN_x film continues to serve as an effective etch stop for KOH etching of Si. The localized damage could be converted into a larger-scale pattern by using a hard mask or by rastering of the lighter

https://dx.doi.org/10.1021/acsanm.0c00248
ACS Appl. Nano Mater. 2020, 3, 2969−2977

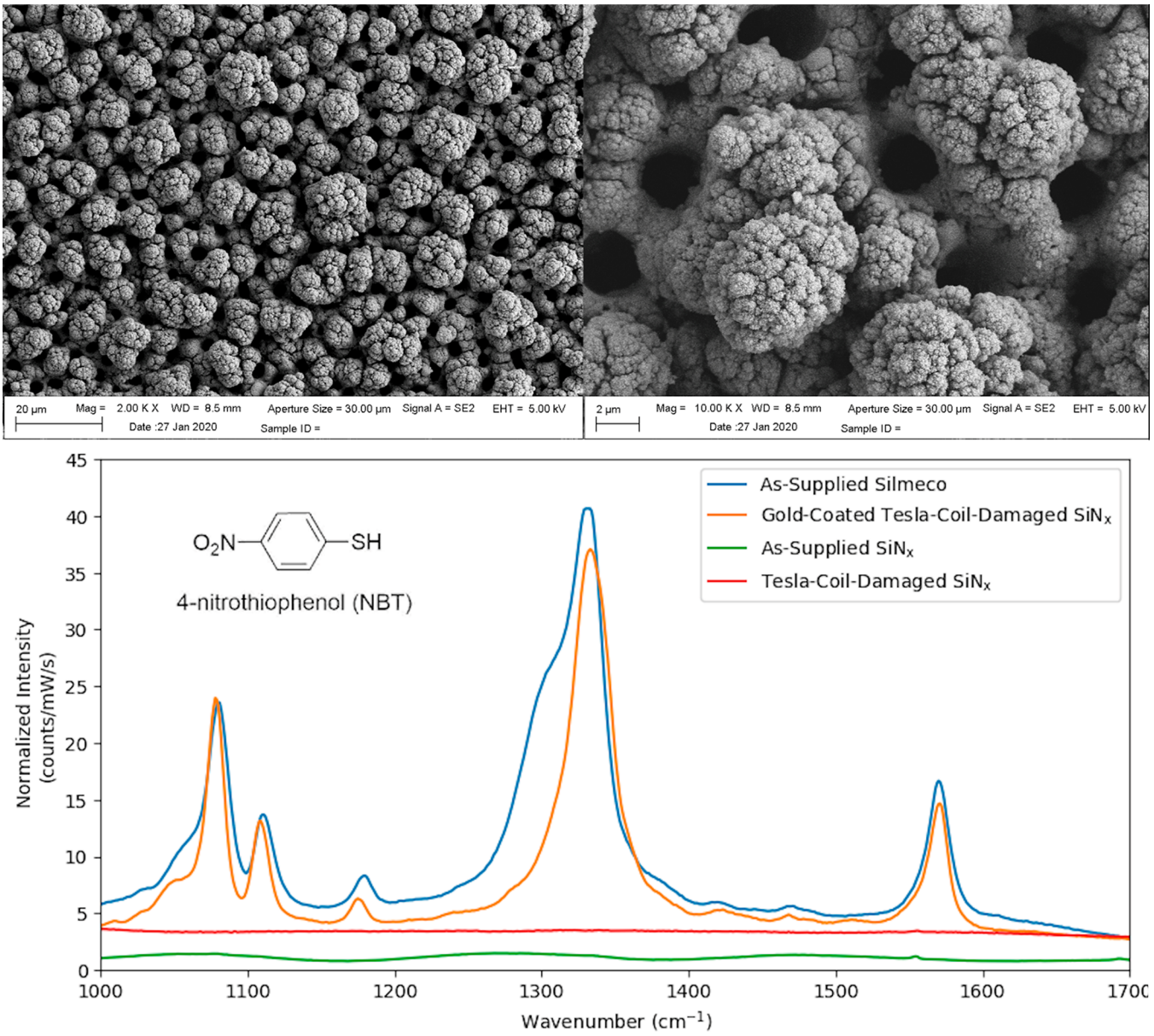

Figure 6. Top: SEM images of Tesla-coil damaged SiN_x after gold coating. Tesla-coil exposure was by Scheme 1c (~90 s exposure at 1 mm electrode distance) and gold coating was by sputtering for 20 s. Voids and surface texture are evident at lower magnification (left), and the presence of grains on a number of length scales is evident at higher magnification (right). Bottom: Using identical spectrometer settings and 1.6 ppm analyte concentrations, the maximum signal intensity from the Tesla-coil-prepared substrate was nearly identical to the signal intensity produced using the commercial nanopillar array substrate prepared by reactive ion etching. No SER spectra were detected from the as-supplied SiN_x-coated chips and gold-free Tesla-coil-damaged chips.

across the surface. For suitable targets, the Tesla-coil approach thus effectively replaces a much more complicated, labor-, time-, and equipment-intensive conventional approach to patterning of these materials that otherwise may require photolithography and RIE. Earlier work[13] had established that with a suitable, simple implementation, the Tesla-coil lighter can be used to form nanoscale structures through a largely stochastic process.[22] The present work shows its ability to deterministically modify existing nanostructures on a larger scale, such as patterning and establishing vias through thin films of SiN_x, thus serving as a low-barrier adjunct to traditional micro- and nanofabrication tools and methods. We demonstrated the use of Tesla-coil patterning to deliver two different applications. The first was the formation of a microscale fluid channel within the bulk silicon wafer underlying the SiN_x thin film. The 170 μm lateral dimension of the channel was controlled by the glass slide masks and Tesla-coil discharge extent while the 160 μm depth was controlled by the wet etching time. The second was the fabrication of a SERS substrate by using Tesla-coil exposure to provide the necessary substrate surface structure, and simple sputter deposition of an essentially unstructured gold thin film to provide the coinage metal surface. SERS enhancement was generated by gold-coating damage marks, and thus the location of enhancement could be readily controlled. Detection of a canonical test molecule, NBT, was demonstrated at a concentration of 1.6 ppm. Similar total signal was detected from both a delicately nanostructured commercial SERS

https://dx.doi.org/10.1021/acsanm.0c00248
ACS Appl. Nano Mater. 2020, 3, 2969−2977

substrate and the substrate fabricated from a Tesla-coil-damaged chip. The Tesla-coil thus holds substantial potential in the hands of practitioners needing only simple tools to create or modify micro- and nanostructures without the barriers to entry or practice of more conventional fabrication methods and tools.

■ ASSOCIATED CONTENT

Supporting Information

The Supporting Information is available free of charge at https://pubs.acs.org/doi/10.1021/acsanm.0c00248.

Scanning electron micrographs and elemental analysis of Tesla-coil damage spots and structures, photographs of damage to copper grids, and scanning (PDF)

■ AUTHOR INFORMATION

Corresponding Author

Jason R. Dwyer − *Department of Chemistry, University of Rhode Island, Kingston, Rhode Island 02881, United States;* orcid.org/0000-0002-2938-2888; Email: jason_dwyer@uri.edu

Authors

Brian S. Sheetz − *Department of Chemistry, University of Rhode Island, Kingston, Rhode Island 02881, United States*

Y.M. Nuwan D.Y. Bandara − *Department of Chemistry, University of Rhode Island, Kingston, Rhode Island 02881, United States;* orcid.org/0000-0003-1921-8467

Benjamin Rickson − *Department of Chemistry, University of Rhode Island, Kingston, Rhode Island 02881, United States*

Michael Auten − *Department of Chemistry, University of Rhode Island, Kingston, Rhode Island 02881, United States*

Complete contact information is available at: https://pubs.acs.org/10.1021/acsanm.0c00248

Author Contributions

The manuscript was written through contributions of all authors. All authors have given approval to the final version of the manuscript.

Notes

The authors declare no competing financial interest.

■ ACKNOWLEDGMENTS

The SEM data was acquired at the RI Consortium for Nanoscience and Nanotechnology, a URI College of Engineering core facility partially funded by the National Science Foundation EPSCoR, Cooperative Agreement #OIA-1655221. We are grateful for the assistance of Dr. Irene Andreu of URI in acquiring nanoscale characterizations. This research has been supported by NSF CAREER award CBET-1150085, NSF CHE-1808344, and NSF EPSCoR Cooperative Agreement #IIA-1330406.

■ ABBREVIATIONS

RIE, reactive ion etching
LPCVD, low-pressure chemical vapor deposition
TEM, transmission-electron microscopy
SEM, scanning electron microscopy
SERS, surface-enhanced Raman spectroscopy
ppm, parts per million
EDX, Energy-dispersive X-ray
NBT, 4-nitrothiophenol.

■ REFERENCES

(1) Dwyer, J. R.; Bandara, Y. M. N. D. Y.; Whelan, J. C.; Karawdeniya, B. I.; Nichols, J. W., Silicon Nitride Thin Films for Nanofluidic Device Fabrication. In *Nanofluidics*, 2 ed., Chapter 7; Edel, J.; Ivanov, A.; Kim, M., Eds.; Royal Society for Chemistry, 2016.

(2) *MEMS Materials and Processes Handbook*; Springer US: New York, 2011; p XXXVI, 1188.

(3) Bermudez, V. M.; Perkins, F. K. Preparation and Properties of Clean Si_3N_4 Surfaces. *Appl. Surf. Sci.* **2004**, *235*, 406−419.

(4) Stine, R.; Cole, C. L.; Ainslie, K. M.; Mulvaney, S. P.; Whitman, L. J. Formation of Primary Amines on Silicon Nitride Surfaces: A Direct, Plasma-Based Pathway to Functionalization. *Langmuir* **2007**, *23*, 4400−4404.

(5) Williams, K. R.; Muller, R. S. Etch Rates for Micromachining Processing. *J. Microelectromech. Syst.* **1996**, *5*, 256−269.

(6) Dwyer, J. R.; Harb, M. Through a Window, Brightly: A Review of Selected Nanofabricated Thin-Film Platforms for Spectroscopy, Imaging, and Detection. *Appl. Spectrosc.* **2017**, *71*, 2051−2075.

(7) Fine, D.; Grattoni, A.; Goodall, R.; Bansal, S. S.; Chiappini, C.; Hosali, S.; van de Ven, A. L.; Srinivasan, S.; Liu, X.; Godin, B.; Brousseau, L.; Yazdi, I. K.; Fernandez-Moure, J.; Tasciotti, E.; Wu, H.-J.; Hu, Y.; Klemm, S.; Ferrari, M. Silicon Micro- and Nanofabrication for Medicine. *Adv. Healthcare Mater.* **2013**, *2*, 632−666.

(8) Ciarlo, D. R. Silicon Nitride Thin Windows for Biomedical Microdevices. *Biomed. Microdevices* **2002**, *4*, 63−68.

(9) Eah, S.-K.; Jaeger, H. M.; Scherer, N. F.; Lin, X.-M.; Wiederrecht, G. P. Femtosecond Transient Absorption Dynamics of Close-Packed Gold Nanocrystal Monolayer Arrays. *Chem. Phys. Lett.* **2004**, *386*, 390−395.

(10) Zheng, H.; Claridge, S. A.; Minor, A. M.; Alivisatos, A. P.; Dahmen, U. Nanocrystal Diffusion in a Liquid Thin Film Observed by in Situ Transmission Electron Microscopy. *Nano Lett.* **2009**, *9*, 2460−2465.

(11) Williamson, M. J.; Tromp, R. M.; Vereecken, P. M.; Hull, R.; Ross, F. M. Dynamic Microscopy of Nanoscale Cluster Growth at the Solid-Liquid Interface. *Nat. Mater.* **2003**, *2*, 532−536.

(12) Dwyer, J. R.; Szyc, Ł.; Nibbering, E. T. J.; Elsaesser, T. Note: An Environmental Cell for Transient Spectroscopy on Solid Samples in Controlled Atmospheres. *Rev. Sci. Instrum.* **2013**, *84*, 036101−036101−036101−036102.

(13) Bandara, Y. M. N. D. Y.; Karawdeniya, B. I.; Dwyer, J. R. Push-Button Method to Create Nanopores Using a Tesla-Coil Lighter. *ACS Omega* **2019**, *4*, 226−230.

(14) Karawdeniya, B. I.; Bandara, Y. M. N. D. Y.; Nichols, J. W.; Chevalier, R. B.; Dwyer, J. R. Surveying Silicon Nitride Nanopores for Glycomics and Heparin Quality Assurance. *Nat. Commun.* **2018**, *9*, 3278.

(15) Guo, P.; Martin, C. R.; Zhao, Y.; Ge, J.; Zare, R. N. General Method for Producing Organic Nanoparticles Using Nanoporous Membranes. *Nano Lett.* **2010**, *10*, 2202−2206.

(16) Venta, K.; Wanunu, M.; Drndić, M. Electrically Controlled Nanoparticle Synthesis inside Nanopores. *Nano Lett.* **2013**, *13*, 423−429.

(17) Ierardi, V.; Becker, U.; Pantazis, S.; Firpo, G.; Valbusa, U.; Jousten, K. Nano-Holes as Standard Leak Elements. *Measurement* **2014**, *58*, 335−341.

(18) Savard, M.; Dauphinais, G.; Gervais, G. Hydrodynamics of Superfluid Helium in a Single Nanohole. *Phys. Rev. Lett.* **2011**, *107*, 254501.

(19) Kuiper, S.; van Rijn, C. J. M.; Nijdam, W.; Elwenspoek, M. C. Development and Applications of Very High Flux Microfiltration Membranes. *J. Membr. Sci.* **1998**, *150*, 1−8.

(20) DesOrmeaux, J. P. S.; Winans, J. D.; Wayson, S. E.; Gaborski, T. R.; Khire, T. S.; Striemer, C. C.; McGrath, J. L. Nanoporous Silicon Nitride Membranes Fabricated from Porous Nanocrystalline Silicon Templates. *Nanoscale* **2014**, *6*, 10798−10805.

(21) van Gelder, W.; Hauser, V. E. The Etching of Silicon Nitride in Phosphoric Acid with Silicon Dioxide as a Mask. *J. Electrochem. Soc.* **1967**, *114*, 869−872.

(22) Kwok, H.; Briggs, K.; Tabard-Cossa, V. Nanopore Fabrication by Controlled Dielectric Breakdown. *PLoS One* **2014**, *9*, No. e92880.
(23) Spinney, P. S.; Howitt, D. G.; Smith, R. L.; Collins, S. D. Nanopore Formation by Low-Energy Focused Electron Beam Machining. *Nanotechnology* **2010**, *21*, 375301.
(24) Karawdeniya, B. I.; Bandara, Y. M. N. D. Y.; Whelan, J. C.; Dwyer, J. R. General Strategy to Make an on-Demand Library of Structurally and Functionally Diverse SERS Substrates. *ACS Applied Nano Materials* **2018**, *1*, 960−968.
(25) Bandara, Y. M. N. D. Y.; Karawdeniya, B. I.; Whelan, J. C.; Ginsberg, L. D. S.; Dwyer, J. R. Solution-Based Photo-Patterned Gold Film Formation on Silicon Nitride. *ACS Appl. Mater. Interfaces* **2016**, *8*, 34964−34969.
(26) Murphy, C. J.; Sau, T. K.; Gole, A. M.; Orendorff, C. J.; Gao, J.; Gou, L.; Hunyadi, S. E.; Li, T. Anisotropic Metal Nanoparticles: Synthesis, Assembly, and Optical Applications. *J. Phys. Chem. B* **2005**, *109*, 13857−13870.
(27) Perney, N. M. B.; Baumberg, J. J.; Zoorob, M. E.; Charlton, M. D. B.; Mahnkopf, S.; Netti, C. M. Tuning Localized Plasmons in Nanostructured Substrates for Surface-Enhanced Raman Scattering. *Opt. Express* **2006**, *14*, 847−857.
(28) Tabatabaei, M.; Najiminaini, M.; Davieau, K.; Kaminska, B.; Singh, M. R.; Carson, J. J. L.; Lagugné-Labarthet, F. Tunable 3d Plasmonic Cavity Nanosensors for Surface-Enhanced Raman Spectroscopy with Sub-Femtomolar Limit of Detection. *ACS Photonics* **2015**, *2*, 752−759.
(29) Yang, L.; Yan, B.; Premasiri, W. R.; Ziegler, L. D.; Negro, L. D.; Reinhard, B. M. Engineering Nanoparticle Cluster Arrays for Bacterial Biosensing: The Role of the Building Block in Multiscale SERS Substrates. *Adv. Funct. Mater.* **2010**, *20*, 2619−2628.
(30) Schmidt, M. S.; Hübner, J.; Boisen, A. Large Area Fabrication of Leaning Silicon Nanopillars for Surface Enhanced Raman Spectroscopy. *Adv. Mater.* **2012**, *24*, OP11−OP18.
(31) Gopinath, A.; Boriskina, S. V.; Reinhard, B. M.; Dal Negro, L. Deterministic Aperiodic Arrays of Metal Nanoparticles for Surface-Enhanced Raman Scattering (SERS). *Opt. Express* **2009**, *17*, 3741−3753.
(32) Stiles, P. L.; Dieringer, J. A.; Shah, N. C.; Van Duyne, R. P. Surface-Enhanced Raman Spectroscopy. *Annu. Rev. Anal. Chem.* **2008**, *1*, 601−626.
(33) Wu, K.; Rindzevicius, T.; Schmidt, M. S.; Mogensen, K. B.; Hakonen, A.; Boisen, A. Wafer-Scale Leaning Silver Nanopillars for Molecular Detection at Ultra-Low Concentrations. *J. Phys. Chem. C* **2015**, *119*, 2053−2062.

https://dx.doi.org/10.1021/acsanm.0c00248
ACS Appl. Nano Mater. 2020, 3, 2969−2977